Study of the Nucleating Effect of Nanozirconia Obtained by Green Synthesis on Low-Density Polyethylene (LDPE)

Felipe Zanette da Silveira[a,b] (iD), *Márcio Antônio Fiori*[c,d,e] (iD), *Tiago Elias Allievi Frizon*[f] (iD),

Luiz Fernando Belchior Ribeiro[f] (iD), *Gustavo Lopes Colpani*[d,e] (iD), *Humberto Gracher Riella*[a*]

[a]Universidade Federal de Santa Catarina (UFSC), Centro Tecnológico, Departamento de Engenharia Química e de Alimentos, 88040-900, Florianópolis, SC, Brasil.
[b]Universidade do Extremo Sul Catarinense (UNESC), Departamento de Engenharia de Materiais, 88806-000, Criciúma, SC, Brasil.
[c]Universidade Tecnológica Federal do Paraná (UTFPR), Laboratório de Ciência e Tecnologia de Materiais (LCTM), Departamento de Física, Pato Branco, PR, Brasil.
[d]Universidade Comunitária da Região de Chapecó (Unochapecó), Programa de Pós-Graduação em Ciências Ambientais (PPGCA), Chapecó, SC, Brasil.
[e]Universidade Comunitária da Região de Chapecó (Unochapecó), Programa de Pós-Graduação em Tecnologia e Gestão da Inovação (PPGTI), Chapecó, SC, Brasil.
[f]Universidade Federal de Santa Catarina (UFSC), Departamento de Energia e Sustentabilidade, 88905-120, Araranguá, SC, Brasil.

The work evaluated the nucleating effect of nanometric zirconia (Zr-NP), obtained by the green sol-gel synthesis route using Euclea natalensis root extract as a reductant, in the low-density polyethylene (LDPE). The Zr-NP was characterized with x-ray diffraction (XRD) and transmission electron microscopy (TEM) which confirmed the presence of Zr-NP in the cubic crystalline phase with an average particle size of 6.73 nm. The Zr-NP was incorporated into the polymeric matrix by solubilization in concentrations ranging between 0 wt% and 6 wt%. Non-isothermal DSC analyzes demonstrated that a small addition of 1 wt% changes the degree of crystallinity from ~23% to ~56%, an increase of ~137%. The addition of Zr-NP also caused a small increase in crystallization and melting temperatures, and a large increase in the total crystallization time of LDPE.

Keywords: *Degree of crystallinity; Crystallization; Thermal transitions; Additives; Nucleating agent; Non-isothermal crystallization.*

1. Introduction

The development of nucleating agents (NA) for polymers is of great technological and industrial importance. The addition of these agents facilitates the nucleation process[1] and improve mechanical performance[2,3], optical[4] and dimensional stability of products made of polymeric materials. The nucleating agents directly influence the degree of crystallinity, the size and quantity of the spherulites, the kinetics and crystallization energy. These effects define the properties of the polymers and interfere with manufacturing processes[5,6].

The nucleating action of inorganic particles has been studied for a long time. Inorganic compounds such as talc[7], silica[8], and metal oxides[9], are extensively studied and applied. However, due to their ionic nature, these materials are difficult to disperse. This factor results in the formation of cluster and the need to use coupling agents that facilitate dispersion in polymer matrices[1-5,10-12].

Zirconia is a ceramic material and can be found in three different crystalline phases: tetragonal, monoclinic and cubic; or even in the amorphous state. The differentiation of the crystalline structure of zirconia is dependent on the synthesis conditions, the calcination temperature and the reagents used[13-15]. Nano zirconia can be obtained by hydrothermal synthesis[16-22], sonochemistry[23,24] or Sol-Gel[25-30]. Recent studies use reagents that are less harmful to the environment and produce nano zirconia particles with dimensions that can reach 5 nm using citric acid, glucose, fructose, maltose, sucrose or plant extract as a reducing agent[13,31]. These routes are called "Green synthesis".

Natal gwarri or Natal ebony (Euclea natalensis) is a tree of African origin that has naphthoquinones and terpenes in its composition. The presence of naphthoquinones in the composition favors the reduction of metals during synthesis, making the extract of this root a promising reagent for green synthesis[13].

Studies show that the addition of zirconia in polymeric matrices causes an increase in strength, Young modulus, hardness, and steady-state wear rate[11,32-34]. These zirconia-containing polymers can be applied in metal protection systems[35,36], dental prostheses[2], or in other applications that require good mechanical and wear resistance. Studies show

*e-mail: humberto.riella@ufsc.br

that the incorporation of zirconia causes an increase in the crystallization temperature (Tc), at glass transition temperature (Tg) and indicate possible changes in the crystallinity of various resins, such as ABS[37], PMMA[38], LLDPE[11] e HDPE[39].

The changes in the physical and thermal properties described in the studies show that zirconia has interesting characteristics to be applied as a nucleation agent of polymeric materials. The good thermal stability under the conditions used in the processing of polymeric materials and its chemical stability make zirconia a promising nucleating additive for the polymer materials processing industry[40-42]. Based on the promising indications already mentioned, this study investigates the use of nano zirconia (Zr-NP) obtained via the green route as a nucleating agent in low-density polyethylene (LDPE).

2. Materials and Methods

2.1. Materials

Zirconium oxychloride was used as a precursor of the zirconia nanoparticles ($ZrOCl_2 \cdot 8H_2O$) (Neon - Brasil). As a reducing agent, the *Euclea natalensis* root extract was collected in Maputo, Mozambique. The root's identity was confirmed by biologist Suzana Macuvele from the Museu de História Natural-UEM. The polymeric matrix used was the low-density polyethylene (LDPE EB853) produced by Brasken with a Melt Flow Index of 2.7 g/10min and density of 0.923g/cm³.

2.2. Experimental

2.2.1. Green synthesis of zirconia nanoparticles

The preparation of nano zirconia started with the production of *Euclea natalenses* extract used as a reducer in the synthesis process. The root was washed with plenty of distilled water, dried at 60 ºC for 24 hours in an oven, and then crushed in the mill with a 5 mm sieve. After milling, the root presented fibrous shapes with approximately 5 mm in length. Subsequently, the root was maintained with mechanical agitation at 80 ºC for 1 hour in a 75 g/L distilled water solution. Finally, the system was vacuum filtered with filter paper and the resulting solution was called root extract.

For the synthesis, the methodology adapted from Silva et al.[13] was employed. For this, a 300 ml aqueous solution with 0.2 mol/L zirconia oxychloride was prepared in a glass reactor and maintained under mechanical agitation at room temperature. *Euclea natalenses* root extract was added with a flow rate of 3.5 mL/min to the solution for three hours. The resulting precipitate was extracted with the vacuum filtration process and then dried in an oven at 105 ºC for 24 hours. It was then calcined at 600 ºC for three hours in a muffle furnace and subsequently deagglomerated by maceration. At the end of the process, zirconia nanoparticles were obtained.

The crystalline structure of zirconium oxide nanoparticles was characterized with X-Ray Diffraction (XRD: RIGAKU MiniFlex600) after the calcination process. The Rietveld method was employed for the identification and quantification of the crystalline phases and the Scherer method was employed to estimate the average crystallite size of the zirconia structures[13,43,44].

The Scanning Electron Microscopy (SEM: Jeol JSM-6390) technique was employed to study the morphology of zirconia clusters and nanoparticles after the calcination process. The studies with SEM were performed with 15 keV beam energy and with different magnifications. At the same time, the energy dispersive technique of x-ray fluorescence (EDS) was employed for chemical identification in the samples. In these procedures, Zr-NP were ultrasonically dispersed in ethyl alcohol and dispersed in the sample holder, where they were then coated with gold to ensure electrical conduction.

For more detailed studies of the shape and average size of Zr-NP, the Transmission Electron Microscopy (TEM: JEM-1011) technique was used. In this procedure, Zr-NP were ultrasonically dispersed in ethyl alcohol and dispersed in the sample holder.

2.2.2. Incorporation of zirconia nanoparticles into LDPE

To incorporate the Zr-NP into the LDPE matrix, the polymer was first solubilized in toluene (Synth – 99%), at a temperature of 90 ºC under mechanical agitation. After total solubilization, the respective amount of Zr-NP was added, and the system was kept under agitation until solidification. Subsequently, the toluene was extracted in an oven at a temperature of 60 ºC for 24 hours. When the extraction is finished, the LDPE film containing Zr-NP is ready.

For the study, 7 different samples were produced, varying the percentage of nano zirconia added to the polymer matrix from 0% to 6% by weight: These were coded as "0x"; where x represents the percentage of zirconia incorporated into the LDPE. The DSC analyses were performed in triplicates, and the 1st and 2nd repetition of the samples were named "0x-01" and "0x-02", respectively. The Table 1 presents the complete planning with the samples and repeats applied to the DSC. The films obtained with different concentrations were divided and sent for characterization.

The Fourier Transform Infrared Spectroscopy (FTIR) technique (Bruker) was used to evaluate the occurrence of important chemical reactions between the Zr-NP and the LDPE matrix.

The dispersion of Zr-NP in the LDPE matrix was performed using the Scanning Electron Microscope - Field Emission Gun (SEM-FEG: Magellan 400 L FEG). The samples are gold-coated to ensure electrical conduction and analyzed with beam energy of 2.0 and 5.0 keV and at different magnifications.

LDPE samples containing different percentages of Zr-NP were evaluated with Differential Scanning Calorimetry (DSC: Perkin Elmer). The thermograms were obtained with two thermal cycles in the temperature range of 35 ºC to 180 ºC, with a nitrogen atmosphere, with a heating rate of 10 ºC/min and a cooling rate of 5 ºC/min. The tests were performed in triplicates for each composition. The thermograms of the second thermal cycle were analyzed to determine the temperatures at the beginning and end of the crystallization and fusion process, and the values of the respective enthalpies of crystallization and fusion.

The degree of crystallinity was determined from the enthalpy values obtained from the thermograms of the second thermal cycle of the DSC by Equation 1[45,46]. The reference

Table 1. Name and composition of the samples studied. DSC analyzes were analyzed in triplicate (sample, 1st repetition, and 2nd repetition). The "x" in the sample nomenclature represents the concentration of nano zirconia.

Sample	Additional Sample for DSC		LDPE (Wt%)	Zr-NP (Wt%)
	1st repetition	2nd repetition		
00	00-1	00-2	100%	0%
01	01-1	01-2	99%	1%
02	02-1	02-2	98%	2%
03	03-1	03-2	97%	3%
04	04-1	04-2	96%	4%
05	05-1	05-2	95%	5%
06	06-1	06-2	94%	6%

value for enthalpy of melting of the material with 100% crystallinity ($\Delta H_m°$) was 290 J/g[1].

$$X_c = \frac{\Delta H_m}{\left[1 - \varnothing\right]\Delta H_m^0} \times 100 \qquad (1)$$

Relative crystallinity (X_t) demonstrates the evolution of the material's crystallinity with respect to time. Its determination is made by fractionating the crystallization peak of the material at intermediate times to determine crystallinity of the polymer at each "t" time[44,47]. Equation 2 was used to calculate X_t.

$$X_t = \frac{\int_{T_0}^{T} \left(\frac{dH_c}{dT}\right)dT}{\Delta H_c} \qquad (2)$$

Where the numerator represents the partial enthalpy of crystallization generated in the arbitrary time interval "T", and the denominator represents the total enthalpy of crystallization.

The LDPE polymer film with different concentrations of Zr-NP was manually cut into small squares of approximately 3 mm. With the aid of an analytical balance, 0.2 g of the material was separated and formed between two PTFE sheets with a constant force of 4000 kgf at a temperature of 190 °C for 30 seconds. After forming, the film obtained was cooled by submersion in water at 10 °C. This procedure was repeated for all concentrations of Zr-NP studied, giving rise to films with an average thickness of 0.067 mm with S.D of 0.007. The films with different concentrations of Zr-NP were characterized by X-Ray Diffraction (XRD: RIGAKU MiniFlex600). The diffractograms were evaluated and the crystallinity of LDPE was determined by Equation 3[48]. The X_c^{XRD} values obtained were evaluated using the 95% confidence interval method.

$$X_c^{XRD} = \frac{A_c}{A_a + A_c} \times 100 \qquad (3)$$

3. Results and Discussions

3.1. Characterization of nano zirconia

The material obtained in the synthesis was calcined at a temperature of 600 °C in a muffle furnace. The temperature adopted for the calcination process was based on studies by Dwivedi et al. [27], da Silva et al. [13] e Bashir et al.[44].

The calcined samples were analyzed with scanning electron microscopy (SEM) and their micrographs are presented in Figure 1 (a) and (b) with magnifications of 50x and 9000x respectively. The micrographs of the material after calcination reveal the formation of large agglomerates made up of small particles. The EDS of region 1 demarcated in Figure 1 (a) reveals the presence of oxygen and zirconia, while the EDS made punctually in the small cluster marked in Figure 1 (b) indicated the presence of zirconia and oxygen together with carbon and calcium. The presence of these unexpected elements is attributed to residues of the calcination process and may be associated with the use of *Euclea natalenses* root extract in the synthesis of the nanoparticle.

Transmission electron microscopy (TEM) images are presented in Figure 2 and confirm that the clusters are formed by nanoparticles with an average size of 6.7 nm. Figure 2 (a) shows the formation of nanometer-sized particles, while Figure 2 (b) shows a unimodal distribution for nanoparticle size.

Figure 3 shows the X-ray diffractogram obtained with the zirconia compound after the calcination process. The diffractogram shows peaks of 2Theta equal to 30.18°, 34.93°, 50.36°, 59.94°, 62.89° and 74.68° associated respectively with planes (111), (200), (220), (311), (222) and (400) of the cubic crystal structures of zirconia (JCPDS No. 27–0997)[13,49,50]. The Rietveld method confirms the presence of zirconia with amorphous phase and cubic crystalline phase, in the percentages of 36.59% and 55.94%, respectively. Using the Scherer method[1-3] the mean of crystallite size determined was 8.74 nm.

The FTIR spectrum can be seen in Figure 4, where bands can be observed in the region from 900 cm-1 to 1150 cm-1 (Region 1) characteristic of zirconia. These bands were also reported by Dwivedi et al.[27] and da Silva et al.[13]. The band observed at 3380 cm-1 and 1630 cm-1 respectively indicates the presence of water and a possible presence of carbonyl from the root extract used in the synthesis of Zr-NP[4,5].

The microscopy results combined with X-ray fluorescence emission spectroscopy and X-ray diffraction prove the formation of Zr-NP with cubic crystalline structures of sizes less than 10 nm. Similar results were obtained by da Silva et al.[13], who reported Zr-NP with sizes ranging between 5.9 nm and 8.54 nm using the sol-gel synthesis method on which this work was based.
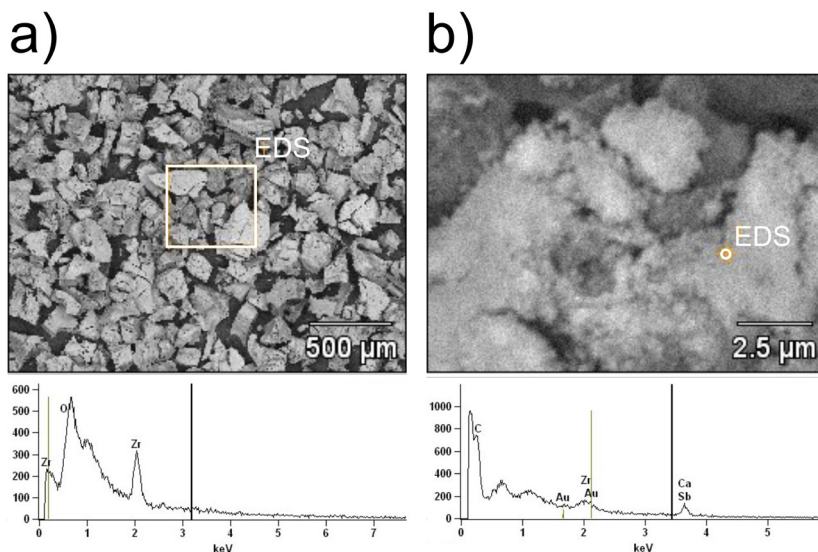
Figure 1. Scanning electron microscopy (SEM) images of zirconia particles after calcination. (a) clusters of particles at 50x magnification, highlighting region "1" analyzed by EDS. (b) surface of a cluster at 900x magnification highlighting point "1" analyzed by EDS.

Bashir et al.[44] used the sol gel method with zirconium oxychloride precursor and ammonia-reducing agent to obtain Zr-NP with dimensions ranging from 8 nm to 75 nm. Zr-NP was subjected to different calcination temperatures ranging from 100 ºC to 1000 ºC. The calcined Zr-NP showed tetragonal and monoclinic crystalline structures in phase proportions that varied with the calcination temperature used. Phase quantification also revealed a proportion of amorphous Zr-NP that ranged from 39.3% to 89.3% depending on the calcination temperature used. These results demonstrate that the percentage of amorphous material obtained by the green route used is very similar to other synthesis processes described in the literature. In general, the green synthesis route used in this work proved to be quite satisfactory, originating cubic Zr-NP with a crystalline percentage greater than 50% and average dimensions below 10 nm.

3.2. Characterization of LDPE with different Zr-NP concentrations

3.2.1. Fourier transform infrared spectroscopy (FTIR) of the polymer

The FTIR spectra of the films obtained by the solubilization process showed typical transmittance bands at 2900 cm^{-1} and 2800 cm^{-1} (CH$_2$), 1450 cm^{-1} (CH) and 710 cm^{-1} (CH2), characteristic of low-density polyethylene[47]. The presence of Zr-NP in the sample could not be observed in the spectrogram due to the low percentages incorporated[51]. The spectra are presented in Figure 5 and did not show significant changes that prove changes in the polymeric structure caused by the presence of Zr-NP.

- Field Emission Gun – Scanning Electron Microscope (FEG-SEM):

LDPE films produced by solubilization with 3 wt% and 6 wt% Zr-NP were analyzed with scanning electron
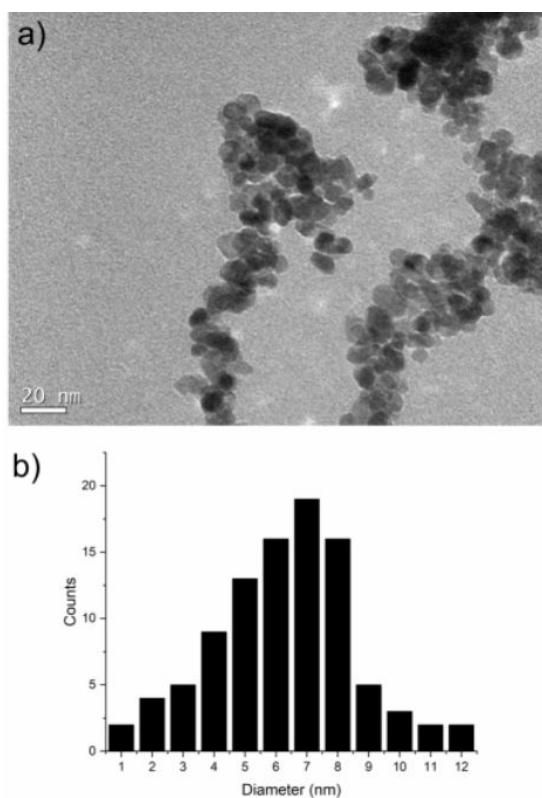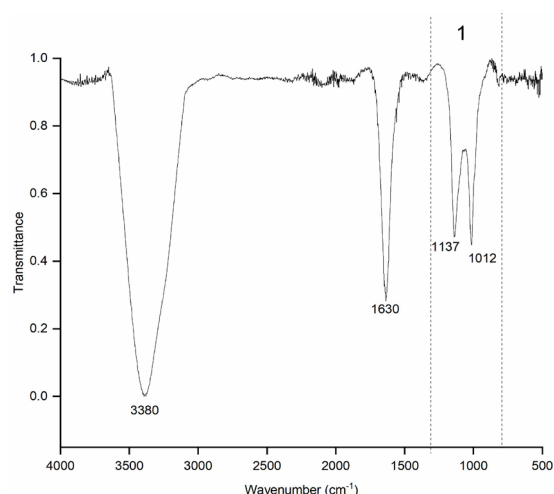

Figure 2. (a) Micrograph obtained with transmission electron microscopy (TEM) for the zirconia compound after the calcination process. (b) Particle size distribution obtained from TEM image analyses.

microscopy (SEM-FEG). Figure 6 (a) shows the LDPE surfaces without significant clusters in the polymer matrix. Figure 6 (b) demonstrates that LDPE with 6% Zr-NP has
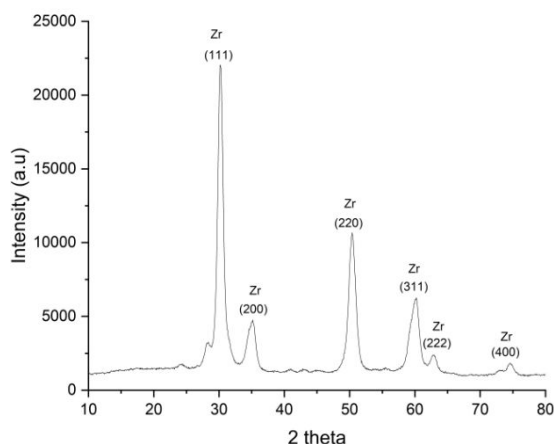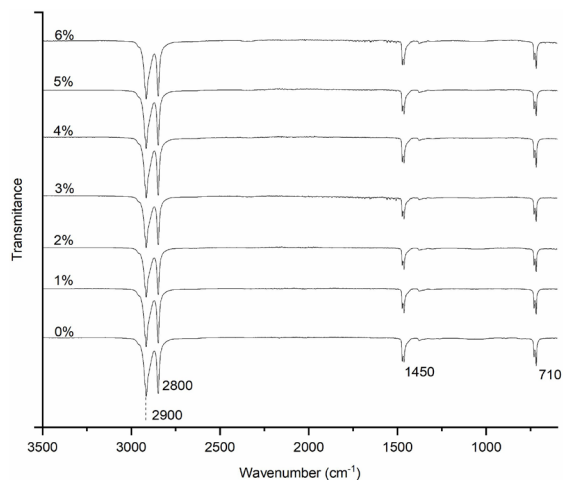
Figure 3. X-ray diffractogram of nanoparticles. Highlighted are the peaks related to the occurrence of Zr-NP and its crystallographic planes.

Figure 5. FTIR spectrum of LDPE with different concentrations of Zr-NP made by solubilization.

Figure 4. FTIR spectrum of Zr-NP. Highlighting region "1" characterized by the presence of Zr-NP.

a greater number of clusters in the LDPE matrix, and the Figure 6 (c) shows an image with greater magnification and highlighting the voids observed on the surface (R1).

SEM-FEG images obtained from a cross section at the sample edge of an LDPE film containing 1 wt% Zr-NP confirm the presence of clusters consisting of Zr-NP and distributed in the polymer matrix (Figure 7 a). Figure 7 (b) shows, at 30,000x magnification, the presence of clusters with varying dimensions, between 50 nm and 3 μm, distributed throughout the polymer matrix. A higher magnification of this region can be observed in Figure 7 (c), which shows a cluster of the R2 region with magnifications of 200,000x, showing the presence of multiple Zr-NP particles in its structure. It is notorious that there is no good physical interaction between the clusters and the polymer matrix, because there are no indicators of coating (or involvement) of these particles by the polymeric matrix. The increase in the number of clusters present in the samples was expected along with the increase in the Zr-NP concentration of the

sample. This increase is caused by the addition of a greater number of clusters resulting from the poor deagglomeration of the material before incorporation, or due to the difficulty in dispersing the Zr-NP in the LDPE due to the chemical incompatibility of the species and the small size of the particles obtained[11,12]. This incompatibility, together with the large amount of clusters present, caused many voids on the surface. Its occurrence is always observed in regions close to the cluster. The micrograph of LDPE with 3% Zr-NP showed the formation of smaller and lower frequency clusters. In the region observed, this sample did not present a void on the surface. These results show that the maximum concentration of Zr-NP should be 3 wt%, as greater additions can lead to the formation of voids in the LDPE matrix as observed for 6 wt% Zr-NP. Difficulty in dispersion and formation of void on the surface was also observed by Kumar et al.[11] by dispersing Zr-NP in an LLDPE/LDPE/PLA/MA-g-PE polymeric matrix. In their study, it was observed that the concentration of 2% Zr-NP resulted in the occurrence of these voids in the polymer matrix.

### 3.2.2. Differential scanning calorimetry (DSC)

LDPE films containing different percentages of Zr-NP were subjected to thermal analysis with DSC. The analyses were performed with two subsequent thermal cycles of heating and cooling, with a heating rate of 10 ºC/min and a cooling rate of 5 ºC/min. The thermograms are shown in Figure 8 and demonstrate that the energies involved in the fusion and crystallization of LDPE are affected by the concentration of Zr-NP, with the addition of this increasing the energy involved in the processes. It can be noted that for both phenomena the biggest difference occurs between the sample with 0% and 1% Zr-NP where the fusion and crystallization energy undergo a large variation. The thermograms also show an increase in crystallization and melting temperatures when adding Zr-NP to LDPE.

Table 2 shows the mean values of the melting temperature (T_m) and crystallization (T_c). The Tukey test demonstrates that the values of crystallization and melting temperature are significantly modified with the addition of Zr-NP. Both temperatures

Table 2. Means and standard deviation of Onset crystallization temperature, crystallization temperature and melting temperature for different concentrations of Zr-NP.

| Zr-NP	T_c^{OnSet} (ºC)		T_c (ºC)		T_m (ºC)	
	Mean	S.D.	Mean	S.D.	Mean	S.D.
00%	101.40	0.00303	98.07	0.09449	110.10	0.09912
01%	102.57	0.11676	98.82	0.1247	111.66	0.41777
02%	102.72	0.1344	98.91	0.09569	111.45	0.28936
03%	102.85	0.07988	98.99	0.06812	111.68	0.23189
04%	103.14	0.09507	99.11	0.03598	111.56	0.20573
05%	103.16	0.09482	99.11	0.11126	112.01	0.30524
06%	103.25	0.08001	99.29	0.01054	111.69	0.07968
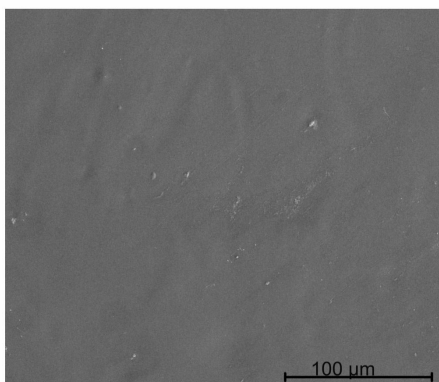
a) LDPE + 3 wt% Zr-NP   b) LDPE + 6 wt% Zr-NP
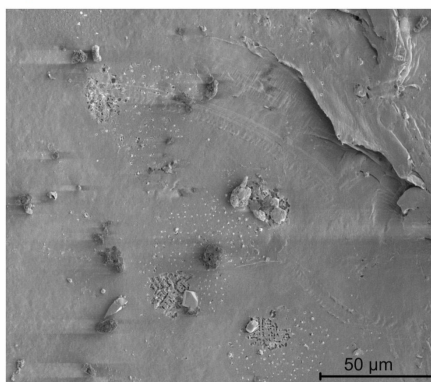
c) LDPE + 6 wt% Zr-NP
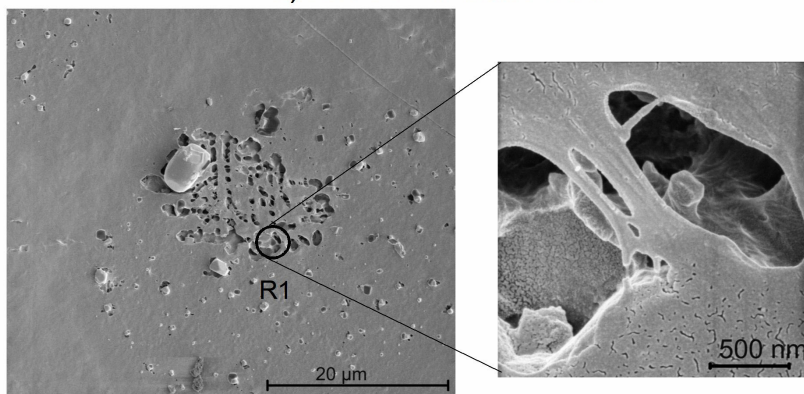
Figure 6. Surface micrograph obtained by SEM-FEG showing the dispersion of nano zirconia in the polymer matrix and the formation of clusters and voids. a) 3 wt% Zr-NP and 1000x magnification; b) 6 wt% Zr-NP and 1600x magnification; C) 6 wt% Zr-NP and 6000x magnification highlight (R1) voids formed in the vicinity of large clusters.

increase with increasing Zr-NP percentage. The average initial crystallization temperature of pure LPDE is 101.4 ºC, and with the addition of Zr-NP it is possible to obtain average values of 103.25 ºC with 6 wt%, an increase of 1.8%. The same occurs with the average crystallization temperature. Pure LDPE has

a value of 98.07 ºC, which rises to 99.29 ºC with the addition of 6% Zr-NP, an increase of 1.2%. Figure 9 shows the average T_c temperature values for the different samples.

The increase in Tc observed by the addition of Zr-NP is small but are still relevant due to the technological
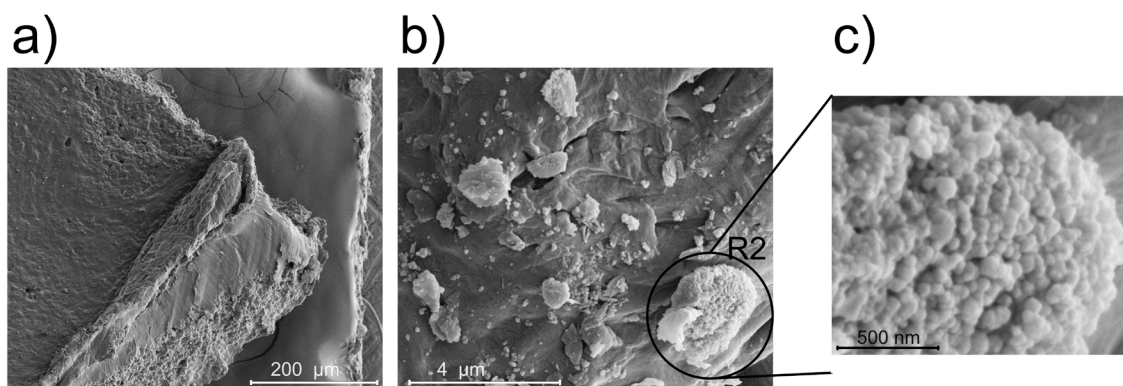
Figure 7. Images obtained from a cross section at the edge of the sample of a LDPE film containing 1% by weight of Zr-NP with: a) magnification of 500; b) magnification of 30,000 highlighting the clusters; c) magnification of 200,000 highlighting the morphology of the cluster.

importance of this parameter. It is observed that the addition of 1.5 wt% nano silver causes an increase of only 0.07 ºC in the T_c of LDPE[52], while sorbitol causes a reduction of approximately 0.07 ºC[53]. These values are better than those observed in this work.

The melting temperatures determined from the thermograms of the second heating cycle also changed significantly with the addition of Zr-NP to LDPE. The Tukey test showed that there was a significant variation in T_m for the concentration of 1 wt% of Zr-NP. Pure LDPE presented a mean value of 110.10 ºC and with the addition of 1 wt% of Zr-NP a mean value of 111.7 ºC, a statistically significant increase of 1.4%. Figure 10 shows the mean T_m values as a function of the percentage of Zr-NP in the LDPE.

3.2.3. Degree of crystallinity

The degree of crystallinity (X_c) of the pure LDPE films and with different concentrations of Zr-NP were calculated from the fusion enthalpy obtained from the DSC thermograms of the second heating with Eq. 1. The degree of crystallinity of films with different concentrations of Zr-NP produced by thermomechanical forming and cooled in water were determined by XRD. Their mean values are shown in Table 3 and Figure 11.
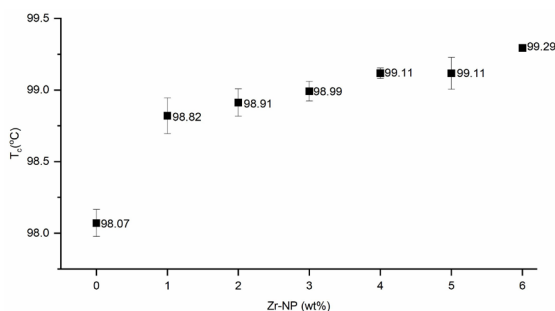
The addition of just 1 wt% of Zr-NP causes an increase in Xc from 23.7% to 56.39%, an increase of ~137%. Additions of 5 wt% cause small change, however the addition of 6% caused a significantly reduction in the crystallinity of LDPE. The reduction of X_c is possibly because of the reduction of the mobility of the polymer chains during the solidification process. The presence of a greater number of clusters observed by microscopy at a concentration of 6 wt% of Zr-NP may be one of the possible causes[11,54,55].

The Figure 12 presents the XRD spectra of the thermally formed and water-cooled LDPE samples. The diffractograms show intensity peaks of 21.8 2theta and 23.46 2theta which correspond respectively to the (110) and (200) planes of the orthorhombic crystalline form of LDPE[48]. Another peak close to 30 2theta referring to the (111) plane of Zr-NP can be observed mainly in samples with higher concentrations of Zr-NP.

The degree of crystallinity of LDPE was determined by analyzing the XRD diffractogram using Eq. 2. The results
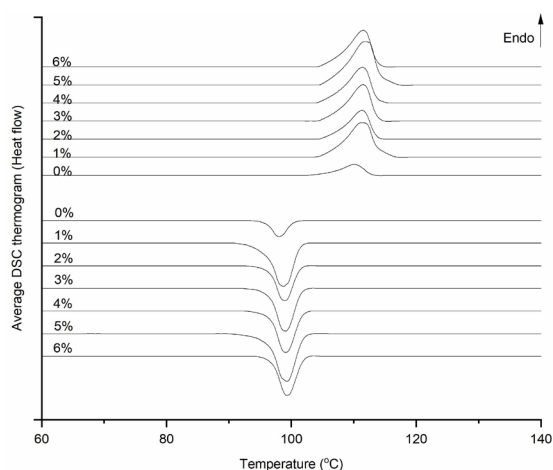
Figure 8. DSC thermograms for LDPE samples with different percentages of Zr-NP in the heating and cooling of the second thermal cycle.
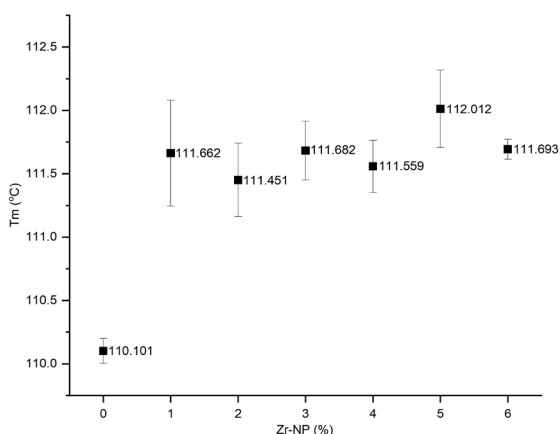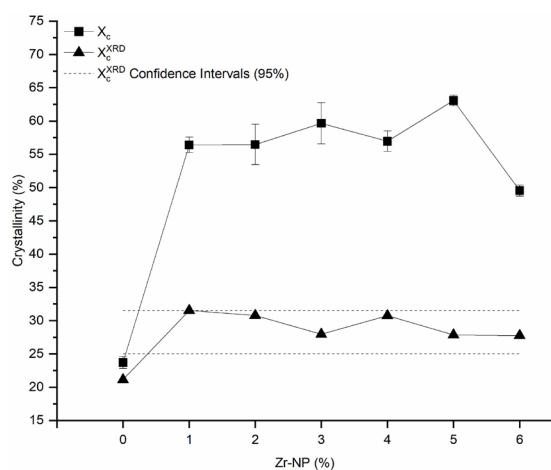

Figure 9. Means crystallization temperatures of LDPE with different concentrations of Zr-NP. highlighting increase in T_c between the pure sample and the sample with 1 wt% Zr-NP.
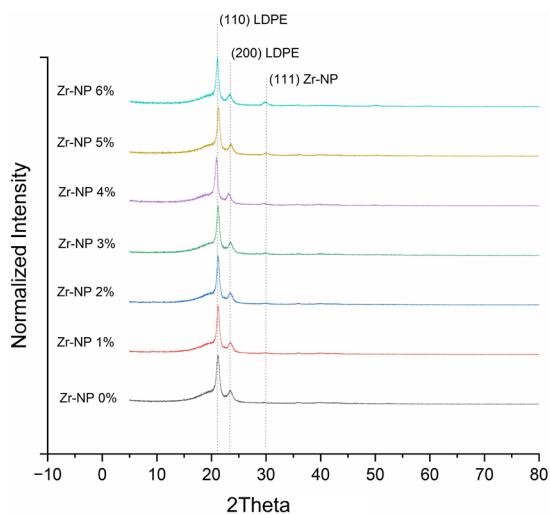
showed that the addition of 1 wt% of Zr-NP causes an increase in the degree of crystallinity of LDPE from 21% to 31%, an increase of 47%. Larger additions of Zr-NP did not

Table 3. Means and standard deviation of the degree of crystallinity of LDPE with different concentrations of Zr-NP.

Zr-NP	ΔH_c		ΔH_m		X_c		X_c^{XRD}
	J.g^{-1}	S.D	J.g^{-1}	S.D	Mean (%)	S.D.	(%)
00%	9.63	2.34	68.50	2.64	23.70	0.53	21.13
01%	33.69	6.42	162.97	3.38	56.39	0.68	31.53
02%	24.88	2.62	163.20	8.79	56.47	1.76	30.79
03%	31.11	2.25	172.39	8.89	59.64	1.78	27.95
04%	30.34	2.40	164.64	4.41	56.96	0.88	30.75
05%	37.22	4.93	182.28	2.29	63.06	0.46	27.87
06%	28.80	1.47	143.23	2.39	49.55	0.48	27.77

Figure 10. Means melting temperatures of LDPE with different concentrations of Zr-NP. Highlighting the increase in T_m between the pure sample and the sample with 1 wt% Zr-NP.

Figure 12. XRD diffraction of the LDPE film cooled in water with different concentrations of Zr-NP.

Figure 11. Degree of crystallinity of LDPE based on the melting enthalpy observed in the DSC thermograms obtained in the second heating cycle for pure LDPE, and the degree of crystallinity of LDPE determined by XRD.

cause a significant difference in the degree of crystallinity. The confidence intervals (95%) of X_c^{XRD} were determined between the limits of 24.99% and 31.51%. When analyzing the data, there is a significant increase in the degree of crystallinity of LDPE when adding Zr-NP. Due to thermal conformation followed by rapid cooling in water, the thermal history of the material analyzed by DSC is different from that analyzed by XRD. For this reason, the results cannot be directly compared.

Several studies involving the addition of Zr-NP in polymeric matrices report alterations in the thermal transitions of the polymeric matrices studied. Kumar et al.[11] observed that the addition of 1.5 wt% Zr-NP in a blend of LLDPE/LDPE/PLA/MA-g-PE caused a 1.8% increase in T_m. In this same study, changes were observed in the mechanical properties of tensile, modulus of elasticity and Haze, these effects are like those caused by the increase in the degree of crystallinity of the matrix. Changes in the T_g of polymeric matrices due to the addition of Zr-NP is also reported in the literature. Amrishraj and Senthilvelan[33] reported a 5% increase in ABS T_g temperature after the addition of 3 wt% nano-zirconia. Similar effect has also been reported for PMMA[40] and epoxy[56]. Although the studies cited do not aim to evaluate the nucleating effect of Zr-NP, the effects reported in the literature were consistent with those observed in the present study for LDPE, where an
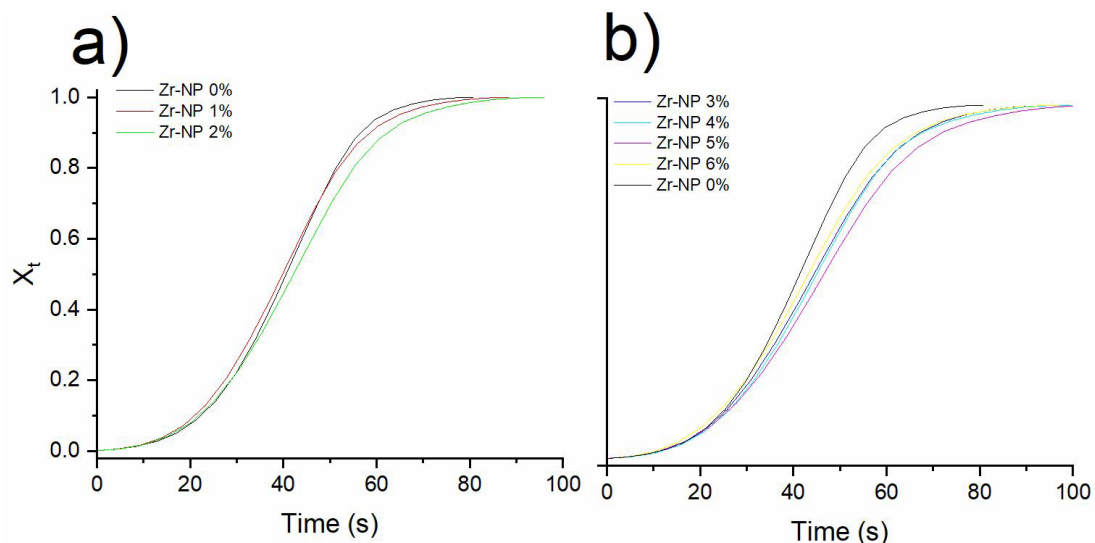
Figure 13. Non-isothermal crystallization curves for different Zr-NP concentrations. a) Comparison of the evolution of crystallinity for samples 00, 01 and 02; b) Comparison of the evolution of crystallinity for samples 00, 03, 04, 05 and 06.

increase in T_m, T_c and the degree of crystallinity caused by the addition of small concentrations of Zr-NP was observed.

### 3.2.4. Relative crystallinity

Relative crystallinity was determined for pure LDPE and LDPE containing different percentages of Zr-NP and the results are presented in Figure 13. The results show that there is a small decrease in the time needed to reach 80% for the sample with 1% of Zr-NP. However, the pure sample crystallize faster for all other conditions studied.

3.2.5. Crystallization half-time ($t_{1/2}$)

The time required to obtain 50% of the total crystallinity of the sample ($t_{1/2}$) was determined and presented in Figure 14. There is a trend of $t_{1/2}$ to increase with increasing concentration up to a level of 5%. The condition with 6 wt% nanoparticles is an exception. In general, the addition of Zr-NP promotes an increase in the time required for the development of the crystallinity of the sample.

The increase in $t_{1/2}$ is an important indicator of changes in crystallization kinetics[57]. The increase in the time required to crystallize the material observed is an indication of a possible reduction in the crystallization kinetics by the addition of Zr-NP up to a percentage limit, in this case up to 6 wt%. Below this percentage limit, the results indicate that Zr-NP induce the nucleation process of the crystalline phases to higher temperatures in the cooling process and, at the same time, increase the $t_{1/2}$. The longer crystallization time can favor the growth of crystals, causing an increase in the degree of crystallinity of the polymer. However, for percentage values above 5 wt% the presence of clusters and voids in the polymer matrix provides antagonistic effects to the crystallization processes.

Considering that the addition of Zr-NP provides important effects on crystallization kinetics, relating parameters of the cooling process with the development of crystallinity
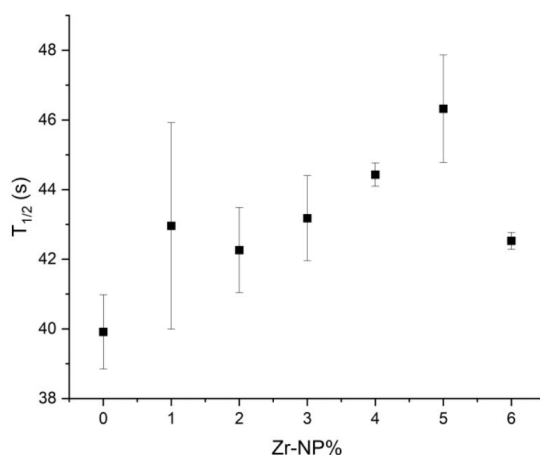
Figure 14. Mean time for LDPE to obtain 50% of its total crystallization ($t_{1/2}$) for different concentrations of Zr-NP.

can provide important information about the crystallization mechanisms of LDPE when combined with nanoparticles. An important parameter is the time required for complete crystallization of LDPE (crystallization time) as a function of Zr-NP concentration.

3.2.6. Total crystallization time (T_t)

The total crystallization time (T_t) can be determined from the DSC thermograms of the samples containing different concentrations of Zr-NP (Table 4). The results indicate that the T_t of LDPE increases with the increase of the percentages of Zr-NP. It is observed that the time to the beginning of the nucleation process of the crystallization phase (t_c^{Onset}) reduces, while the time to the completion of the crystallization process (t_c^{Offset}) is not affected. This effect increases the time for the complete crystallization process
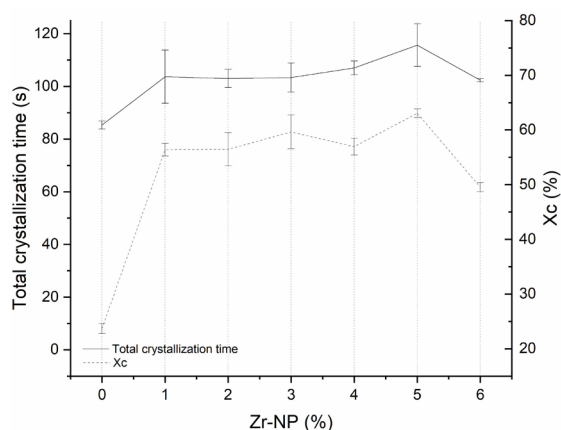
and promotes an increase in the degree of crystallinity. At the same time, it corroborates the hypothesis that Zr-NP acts as a nucleation agent, as they provide the nucleation process in shorter cooling times.

It is notorious that the degree of crystallinity of LDPE is positively affected by Zr-NP, up to the percentage limit of 5 wt%. This effect is possibly due to the reduction in the time of initiation of the nucleation process and the kinetic changes indicated by the increase to $t_{1/2}$. These effects corroborate the capacity of Zr-NP LDPE as a nucleating agent. Figure 15 shows the relationship between the degree of crystallinity (X_c) and "the total time for crystallization" (T_t) for the different Zr-NP concentrations in LDPE. The results show a strong correlation between the time of complete crystallization of LDPE and the degree of crystallinity of the polymer as a function of Zr-NP concentration.

It is notorious that the addition of Zr-NP provides increased time for complete crystallization. With the addition of 3 wt% of Zr-NP the time for total crystallization of LDPE is 111.00 seconds, an increase of 30.59% compared to the pure sample. With this percentage of Zr-NP, LDPE acquires the highest degree of crystallinity, of 0.48, an increase of 140.00% in relation to pure LDPE. These results prove that zirconia (Zr-NP) nanoparticles act as nucleating agents of LDPE.

4. Conclusion

The results show strong evidence that zirconia nanoparticles (Zr-NP) act as a nucleating agent for low-density polyethylene (LDPE), providing greater degrees of crystallinity together with an increase in the crystallization temperature. The addition of small percentages of Zr-NP (1 wt%) makes the time to the complete crystallization process greater, indicating a possible significant change in crystallization kinetics.

With the increase in the percentage, these effects are significantly positive, indicating that it is possible to incorporate percentages between 1 wt% and 5 wt% of Zr-NP and obtain the effect of a nucleating agent. For concentrations above 6 wt% of Zr-NP, the nucleating agent action is reduced. This effect is possibly correlated to the reduction in the mobility of the polymer chains during the solidification process and the presence of a greater number of Zr-NP clusters.

In general, the results show that Zr-NP can be treated as nucleating agents of LDPE and point to a possible and promising nucleating additive for the polymer processing industry.

5. References

1. Niu H, Wang N, Li Y. Influence of β-nucleating agent dispersion on the crystallization behavior of isotactic polypropylene. Polymer (Guildf). 2018;150:371-9.
2. Elmadani AA, Radović I, Tomić NZ, Petrović M, Stojanović DB, Jančić Heinemann R, et al. Hybrid denture acrylic composites with nanozirconia and electrospun polystyrene fibers. PLoS One. 2019;14(12):1-19.
3. Raab M, Ščudla J, Kolařík J. The effect of specific nucleation on tensile mechanical behaviour of isotactic polypropylene. Eur Polym J. 2004;40(7):1317-23.
4. Kristiansen M, Werner M, Tervoort T, Smith P, Blomenhofer M, Schmidt HW. The binary system isotactic polypropylene/bis(3,4-dimethylbenzylidene)sorbitol: phase behavior, nucleation, and optical properties. Macromolecules. 2003;36(14):5150-6.
5. Binsbergen FL. Heterogeneous nucleation in the crystallization of polyolefins: Part 1. Chemical and physical nature of nucleating agents. Polymer (Guildf). 1970;11(5):253-67.
6. Wang W, Zhao G, Guan Y, Wu X, Hui Y. Effect of rapid heating cycle injection mold temperature on crystal structures, morphology of polypropylene and surface quality of plastic parts. J Polym Res. 2015;22(5):1-11.
7. Marco C, Ellis G, Gómez MA, Arribas JM. Comparative study of the nucleation activity of third-generation sorbitol-based nucleating agents for isotactic polypropylene. J Appl Polym Sci. 2002;84(13):2440-50.
8. Li J, He W, Long L, Zhang K, Xiang Y, Zhang M, et al. A novel silica-based nucleating agent for polypropylene: preparation, characterization, and application. Journal of Vinyl and Additive Technology. 2018;24(1):58-67.
9. Zhang YF, Li D, Chen QJ. Preparation and nucleation effects of nucleating agent hexahydrophthalic acid metal salts for isotactic polypropylene. Colloid Polym Sci. 2017;295(10):1973-82.
10. Ambilkar SC, Das C. Surface modification of zirconia by various modifiers to investigate its reinforcing efficiency toward nitrile rubber. Polym Compos. 2023;44(3):1512-21.
11. Kumar R, Upadhyaya PRADEEP, Chand N. Effect of chemically modified nano zirconia addition on properties of LLDPE/LDPE/PLA/MA-g-PE bio-nanocomposite blown films for packaging applications. Int J Phys Sci. 2014;3:2319-26.
12. Ma X, Peng C, Zhou D, Wu Z, Li S, Wang J, et al. Synthesis and mechanical properties of the epoxy resin composites filled with

Table 4. Average total LDPE crystallization times (T_t) obtained from DSC thermograms for concentrations of 0% to 6% Zr-NP.

Zr-NP (%)	T_t (Mean) (s^{-1})	S.D.
0	85.33	1.527
1	103.67	10.066
2	102.99	3.464
3	103.33	5.507
4	107.00	2.645
5	115.67	8.083
6	102.33	0.577

Figure 15. Comparison of the total crystallization time (T_t) obtained from DSC thermograms, and the degree of crystallinity calculated for LDPE with concentrations of 0% to 6% Zr-NP.

sol−gel derived ZrO 2 nanoparticles. J Sol-Gel Sci Technol. 2018;88:442-53.

13. Silva AFV, Fagundes AP, Macuvele DLP, de Carvalho EFU, Durazzo M, Padoin N, et al. Green synthesis of zirconia nanoparticles based on Euclea natalensis plant extract: optimization of reaction conditions and evaluation of adsorptive properties. Colloids Surf A Physicochem Eng Asp. 2019;583(September):123915.

14. Goharshadi EK, Hadadian M. Effect of calcination temperature on structural, vibrational, optical, and rheological properties of zirconia nanoparticles. Ceram Int. 2012;38(3):1771-7.

15. Rahim NH, Lau KY, Muhamad NA, Mohamad N, Tan CW, Vaughan AS. Structure and dielectric properties of polyethylene nanocomposites containing calcined zirconia. IEEE Trans Dielectr Electr Insul. 2019;26(5):1541-8.

16. Ahmad T, Shahazad M, Phul R. Hydrothermal synthesis, characterization and dielectric properties of zirconia nanoparticles. Material Sci & Eng Int. 2017;27(6):5622-7.

17. Fathima JB, Pugazhendhi A, Venis R. Synthesis and characterization of ZrO2 nanoparticles-antimicrobial activity and their prospective role in dental care. Microb Pathog. 2017;110:245-51.

18. Cui H, Li Q, Gao S, Shang JK. Strong adsorption of arsenic species by amorphous zirconium oxide nanoparticles. J Ind Eng Chem. 2012;18(4):1418-27.

19. Prasad MS, Mallikarjun B, Ramakrishna M, Joarder J, Sobha B, Sakthivel S. Zirconia nanoparticles embedded spinel selective absorber coating for high performance in open atmospheric condition. Sol Energy Mater Sol Cells. 2018;174:423-32.

20. Reddy CV, Babu B, Reddy IN, Shim J. Synthesis and characterization of pure tetragonal ZrO2 nanoparticles with enhanced photocatalytic activity. Ceram Int. 2018;44(6):6940-8.

21. Sagadevan S, Podder J, Das I. Hydrothermal synthesis of zirconium oxide nanoparticles and its characterization. J Mater Sci Mater Electron. 2016;27(6):5622-7.

22. Zhu H, Yang D, Xi Z, Zhu L. Hydrothermal synthesis and characterization of zirconia nanocrystallites. J Am Ceram Soc. 2007;90(4):1334-8.

23. Manoharan D, Loganathan A, Kurapati V, Nesamony VJ, Unique sharp photoluminescence of size-controlled sonochemically synthesized zirconia nanoparticles. Ultrason Sonochem. 2015;23:174-84.

24. Zinatloo-Ajabshir S, Salavati-Niasari M. Facile route to synthesize zirconium dioxide (ZrO2) nanostructures: Structural, optical and photocatalytic studies. J Mol Liq. 2016;216:545-51.

25. Bumajdad A, Nazeer A, Al-Sagheer F, Nahar S, Zaki M, Controlled synthesis of ZrO 2 nanoparticles with tailored size, morphology and crystal phases via organic / inorganic hybrid films. Sci Rep. 2018;8(1):1-9.

26. Chakravarty R, Shukla R, Ram R, Tyagi A, Dash A, Venkatesh M, Practicality of tetragonal nano-zirconia as a prospective sorbent in the preparation of 99Mo/99mTc Generator for biomedical applications. Chromatographia. 2010;72(9–10):875-84.

27. Dwivedi R, Maurya A, Verma A, Prasad R, Bartwal KS, Microwave assisted sol – gel synthesis of tetragonal zirconia nanoparticles. J Alloys Compd. 2011;509:6848-51.

28. Majedi A, Davar F, Abbasi A. Citric acid-silane modi fi ed zirconia nanoparticles: Preparation, characterization and adsorbent effi ciency. J Environ Chem Eng. 2018;6:701-9.

29. Tana F, Messori M, Contini D, Cigada A, Valente T, Variola F, et al. Synthesis and characterization of scratch-resistant hybrid coatings based on non-hydrolytic sol-gel ZrO2 nanoparticles. Prog Org Coat. 2017;103:60-8.

30. Santos V, Silveira NP, Bergmann CP. In-situ evaluation of particle size distribution of ZrO2-nanoparticles obtained by sol–gel. Powder Technol. 2014;267:392-7.

31. Kazemi F, Arianpour F, Taheri M, Saberi A, Rezaie HR. Effects of chelating agents on the sol-gel synthesis of nano-zirconia: comparison of the Pechini and sugar-based methods. Int J Miner Metall Mater. 2020;27(5):693-702.

32. Cao W, Gong J, Qi Y, Yang D, Gao G, Wang H, et al. Tribological behavior of Nano-ZrO 2 reinforced PTFE-PPS composites. J Wuhan Univ Technol-Mater Sci Ed. 2019;34:527-33.

33. Amrishraj D, Senthilvelan T. Acrylonitrile butadiene styrene composites reinforced with nanozirconia and PTFE: mechanical and thermal behavior. Polym Compos. 2018;39:E1520-30.

34. Rostamiyan Y, Ferasat A. High-speed impact and mechanical strength of ZrO 2 /polycarbonate nanocomposite. Int J Damage Mech. 2017;26(7):989-1002.

35. Eduok U, Szpunar J, Ebenso E. Synthesis and characterization of anticorrosion zirconia/acrylic nanocomposite resin coatings for steel. Prog Org Coat. 2019;137:105337.

36. Chaudhari S, Patil PP, Mandale AB, Patil KR, Sainkar SR. Use of poly(o-toluidine)/ZrO2 nanocomposite coatings for the corrosion protection of mild steel. J Appl Polym Sci. 2007;106(1):220-9.

37. Amrishraj D, Senthilvelan T. Fracture behavior of acrylonitrile butadiene styrene (ABS) hybrid composites reinforced with nano zirconia and poly tetra fluoro ethylene (PTFE). Trans Indian Inst Met. 2018;71:2251-9.

38. Wang X, Wu L, Li J. Influence of nanozirconia on the thermal stability of poly(methyl methacrylate) prepared by in situ bulk polymerization. J Appl Polym Sci. 2010;117(1):163-70.

39. Nabiyev AA, Olejniczak A, Pawlukojc A, Balasoiu M, Bunoiu M, Maharramov AM, et al. Nano-ZrO2 filled high-density polyethylene composites: Structure, thermal properties, and the influence γ-irradiation. Polym Degrad Stabil. 2020;171:109042.

40. Wang X, Wu L, Li J. Synergistic flame retarded poly(methyl methacrylate) by nano-ZrO 2 and triphenylphosphate. J Therm Anal Calorim. 2011;103(2):741-6.

41. Qi Y, Sun B, Zhang Y, Gao G, Zhang P, Zheng X. Tribological properties of nano-ZrO2 and PEEK reinforced PTFE composites based on molecular dynamics. Lubricants. 2023;11(5):194.

42. Gad MM, Abualsaud R, Rahoma A, Al-Thobity AM, Al-Abidi KS, Akhtar S. Effect of zirconium oxide nanoparticles addition on the optical and tensile properties of polymethyl methacrylate denture base material. Int J Nanomedicine. 2018;13:283-93.

43. Davar F, Majedi A, Mirzaei A. Polyvinyl alcohol thin film reinforced by green synthesized zirconia nanoparticles. Ceram Int. 2018;44(16):19377-82.

44. Bashir M, Riaz S, Kayani ZN, Naseem S. Synthesis of bone implant substitutes using organic additive based zirconia nanoparticles and their biodegradation study. J Mech Behav Biomed Mater. 2018;88:48-57.

45. Canevarolo SV Jr. Ciência dos polímeros: um texto básico para tecnólogos e engenheiros. 2nd ed. São Paulo: Artliber; 2006.

46. Morozo MA, Duarte GW, Silva LL, Mello JMMD, Zanetti M, Colpani GL, et al. A design of experiments approach to analyze the effects of hydroxyapatite and maleic anhydride grafted polyethylene contents on mechanical, thermal and biocompatibility properties of green high-density polyethylene-based composites. Mater Res. 2023;26(suppl. 1):e20220548.

47. Wellen RMR, Rabello MS. Non-isothermal cold crystallization kinetics and morphology of PET + SAN blends. J Appl Polym Sci. 2010;116(2):1077-87.

48. Sousa GS, Kalantar Mehrjerdi A, Skrifvars M, d'Almeida JRM. Thermo-mechanical properties of polyethylene composites filled with soapstone waste. J Appl Polym Sci. 2024;141(9)

49. Guglielminotti E, Boccuzzi F, Pinna F, Strukul G. The effect of potassium addition on the surface chemical structure and activity of supported iron. J Catal. 1997;(167):153-63.

50. Platero EE, Mentruit MP. FTIR characterisation of Re, (CO)10 adsorbed on sulfated zirconium dioxide. Polyhedron. 1997;(20):3489-92.

51. Silva DJ, Wiebeck H. CARS-PLS regression and ATR-FTIR spectroscopy for eco-friendly and fast composition analyses of LDPE/HDPE blends. J Polym Res. 2018;25(5):112.

52. Sahoo RK, Panda BP, Nayak SK, Mohanty S. Mechanical and morphological investigation of virgin polyethylene and silver nanoparticle-loaded nanocomposites film: comprehensive analysis of kinetic models for non-isothermal crystallization. Bull Mater Sci. 2017;40(2):307-20.

53. Li X, Cao Y, Du Q, Yin Y, Tu D. Charge distribution and crystalline structure in polyethylene nucleated with sorbitol. J Appl Polym Sci. 2001;82(3):611-9.

54. Kumar S, Purohit R, Malik MM. Properties and applications of polymer matrix nano composite materials. Mater Today Proc. 2015;2(4-5):3704-11.

55. Suresha B, Padaki A, Jain A, Kumar B, Kulkarni AA. Role of zirconia filler on mechanical properties of HDPE/UHMWPE blend composites. Appl Mech Mater. 2019;895:272-7.

56. Medina R, Haupert F, Schlarb AK. Improvement of tensile properties and toughness of an epoxy resin by nanozirconium-dioxide reinforcement. J Mater Sci. 2008;43(9):3245-52.

57. Ding W, Chu RKM, Mark LH, Park CB, Sain M. Non-isothermal crystallization behaviors of poly(lactic acid)/cellulose nanofiber composites in the presence of CO2. Eur Polym J. 2015;71:231-47.